



ORIGINAL ARTICLE

Adsorption of bentazon on activated carbon prepared from *Lawsonia inermis* wood: Equilibrium, kinetic and thermodynamic studies



Abdesslem Omri *, Ahmed Wali, Mourad Benzina

Laboratory of Water-Energy-Environment (LR3E), Code: AD-10-02, National School of Engineers of Sfax, University of Sfax, BP W, 3038 Sfax, Tunisia

Received 8 December 2011; accepted 27 April 2012
Available online 8 May 2012

KEYWORDS

Activated carbon;
Bentazon;
Adsorption;
Isotherm;
Kinetic;
Thermodynamic

Abstract The adsorption of bentazon onto *Lawsonia inermis* wood-based activated carbon (LWAC) was carried out in this work. The effects of different reaction parameters such as the initial bentazon concentration, contact time, activated carbon dosage, stirring rate, temperature and pH on bentazon adsorption were investigated in a batch process mode. Equilibrium data were analyzed by the Langmuir, Freundlich and Temkin isotherm model. Langmuir isotherm provided the best fit to the equilibrium data with maximum adsorption capacity of 169.49 mg/g at 20 °C. Adsorption kinetic was found to follow the pseudo-second-order kinetic model. The mechanism of the adsorption process was determined from the intraparticle diffusion model. The calculated thermodynamic parameters such as ΔG° , ΔH° and ΔS° showed that the adsorption of bentazon onto LWAC was feasible, spontaneous and exothermic at 20–40 °C. Desorption of the used LWAC was studied using ethanol as solvent and a percent desorption efficiency of bentazon equalizes 73.8% was obtained after three cycles.

© 2012 Production and hosting by Elsevier B.V. on behalf of King Saud University. This is an open access article under the CC BY-NC-ND license (<http://creativecommons.org/licenses/by-nc-nd/3.0/>).

1. Introduction

The use of pesticides coincides with the chemical age, which has transformed society since the 1950s. In areas where inten-

sive monoculture is practiced, pesticide use has been the standard method for pest control. Unfortunately, the use of pesticides can also result in environmental problems, such as disruption of predator–prey relationships and loss of biodiversity. Additionally, the slow degradation of pesticides in the environment can lead to environmental contamination of water, soil, air, several types of crops, and, indirectly, of humans (Navalon et al., 2002). Bentazon is also known by the trade name Basagran. It is a selective post-emergence herbicide used to control many broadleaf weeds and sedges primarily by contact action in most gramineous and many

* Corresponding author. Tel.: +216 96803179.

E-mail address: omriabdesslem@yahoo.fr (A. Omri).

Peer review under responsibility of King Saud University.



Production and hosting by Elsevier

large seeded leguminous crops such as food and feed crops including alfalfa, beans, corn, peanuts, peas, asparagus, cereals, peppers, peppermint, rice and sorghum (Pourata et al., 2009). It is also used on two terrestrial nonfood crops: ornamental lawns and turf. It has little effect on germinating seeds, and is not used pre-emergence. It is harmful if swallowed or absorbed through skin. It causes moderate eye irradiation. So, contact with eye, skin or clothing should be avoided (Garrido et al., 1998). The maximum concentration of bentazon admitted by the World Health Organization (WHO) in drinking water is 30 µg/L (World Health Organisation, 2004), while the USEPA maximum acceptable bentazon concentration in drinking water is 300 µg/L (United States Environmental Protection Agency, 1996).

There are several procedures that were used for pesticides removal from water such as photocatalytic degradation (Aungpradit et al., 2007; Mahalakshmi et al., 2007), combined photo-Fenton and biological oxidation (Ballesteros Martin et al., 2008), advanced oxidation processes (Saritha et al., 2007), aerobic degradation (Rajashekara Murthy and Manonmani, 2007), nanofiltration membranes (Ahmad et al., 2008), ozonation (Maldonado et al., 2006) and adsorption (Ali and Gupta, 2006). Adsorption by activated carbon is one of the most widely used techniques and has proven to be effective in the removal of pesticides from aqueous solutions (Ren et al., 2011). This is due to their mechanical stability, low specificity, fast adsorption kinetics and high adsorption capacities (Halim et al., 2010; Wang et al., 2007).

A variety of carbonaceous raw materials are used for the production of activated carbons. Physical and chemical characteristics of the raw material and the preparation methods have significant effect on the quality and properties of activated carbons (Mourão et al., 2011). Due to high carbon and low ash contents, many of agricultural by-products are appropriate for use as precursors for activated carbon production.

Lawsonia inermis is a shrub or small tree frequently cultivated in dry tropical and subtropical zones, including North Africa, India, Sri Lanka, and the Middle East (Chung et al., 2002). The total area of planted Lawsonia inermis in Tunisia stood at 500 hectares in 2010. Powdered leaves (henna) of this plant are used as a cosmetic for staining hands and hairs (Ali et al., 2009). The dyeing property as well as the UV absorption, antibacterial, antispasmodic, corrosion inhibitors were attributed to the presence of lawsone in henna leaves (Al-Sehaibani, 2000; Dweck, 2002). The Lawsonia inermis wood is used as a source of fuel and it produces a charcoal.

The objective of this work was to study the removal of bentazon from aqueous solutions using activated carbon prepared from Lawsonia inermis wood (LWAC). The adsorbent was prepared and characterized by surface and pore structural characteristics, scanning electron microscopy (SEM) and Fourier transform infrared spectroscopy (FT-IR) analyses. The effects of contact time, initial concentration of bentazon, activated carbon dosage, stirring rate, temperature and initial solution pH were studied. The removal capacity of LWAC was studied by fitting the adsorption data to kinetic and isotherm models. Desorption studies of the used LWAC were also undertaken.

2. Materials and methods

2.1. Materials

Lawsonia inermis wood was collected from the field in Gabes (Tunisia), cut into small pieces of 2–3 cm and dried in sunlight until all the moisture evaporated. After grinding to a fine particle in a steel blender, the Lawsonia inermis wood was sieved to the size of 1–2 mm and dried at 110 °C for 2 h.

Bentazon obtained from BASF Aktiengesellschaft, 67056 Ludwigshafen, Germany, was used as adsorbate. For clarity, the molecular structure of bentazon is shown in Fig. 1. Distilled water was used in adsorption experiments.

2.2. Preparation and characterization of LWAC

Activated carbons were prepared from Lawsonia inermis wood by carbonization under nitrogen flow and activation under water vapor. Carbonization was carried out in a vertical stainless-steel reactor (length 170 mm, interior diameter 22 mm) which was inserted into a cylindrical electric furnace Nabertherm. The dried wood was placed into the reactor and heated from room temperature to 400 °C at a constant heating rate of 10 °C/min under nitrogen flow, then held at 400 °C for 1 h. The samples were left to cool down after the carbonization. Activation was carried out in the same furnace. The charcoal obtained was then physically activated at 850 °C for 2 h under a nitrogen flow (100 cm³/min) saturated in steam after passing through the water saturator heated at 80 °C. The tenor steam was fixed at 0.395 kg H₂O/kg N₂. After activation, the sample was cooled to ambient temperature under N₂ flow rate. The produced activated carbon was then dried at 105 °C overnight, ground and sifted to obtain a powder with a particle size smaller than 45 µm, and finally kept in hermetic bottle for subsequent uses.

The surface area of the LWAC was calculated by BET (Brunauer–Emmett–Teller) equation within the 0.01–0.15 relative pressure range. Micropore volume, micropore area and external surface area were calculated by using the *t*-plot method. The total pore volume was determined from the amount of N₂ adsorbed at a relative pressure close to unity (~0.99) by assuming that the pores are then filled with liquid adsorbate (N₂). All calculations were performed by using the software supplied by Autosorb 1C.

The surface morphology of the samples was examined using a scanning electron microscope (Philips XL30 microscope).

The surface functional groups and structure were studied by FTIR spectroscopy. The FTIR spectra of the LWAC were recorded between 500 and 4000 cm⁻¹ in a NICOET spectrometer.

2.3. Adsorption experiments

All chemicals used in this work, were of analytical reagent grade and were used without further purification. The initial pH of each bentazon solution was adjusted by using 0.1 mol/L NaOH and 0.1 mol/L HCl solutions. Batch equilibrium adsorption experiments were performed using 100 mL of bentazon solution. After adsorption process the adsorbent was separated from the samples by filtering and the filtrate was analyzed using UV-vis spectrophotometer (UV-1650PC

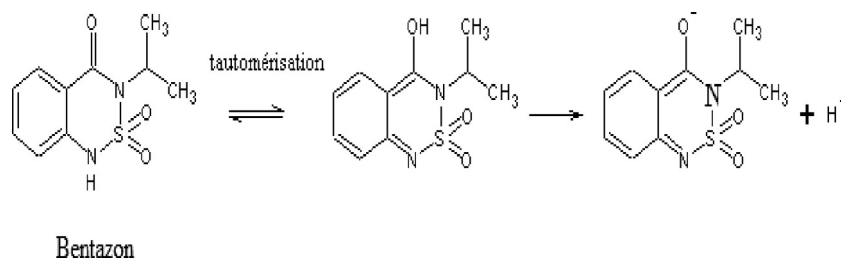


Figure 1 Molecular structure of bentazon, keto-enol tautomerism and dissociation equilibrium.

Shimadzu, Japan) at its maximum wavelength of 232 nm. The effects of adsorption parameters on adsorption of bentazon onto LWAC such as, pH (2.3–11.3), activated carbon dosage (10–70 mg), stirring rate (50–400 rpm), initial bentazon concentration (22–78 mg/L), contact time (5–180 min) and temperature (20–40 °C) were studied. The amount of bentazon adsorbed (q_e) was calculated by using the following mass balance equation,

$$q_e = \frac{(C_0 - C_e) \cdot V}{m} \quad (1)$$

and the removal efficiency of bentazon was calculated as follows:

$$\text{Removal efficiency, } R = \frac{C_0 - C_e}{C_0} \times 100 \quad (2)$$

where C_0 and C_e (mg/L) are the liquid-phase concentrations of bentazon initially and at equilibrium, respectively. V is the volume of the solution (L) and m is the mass of dry adsorbent used (g).

2.4. Fitness of the adsorption kinetic models

The kinetic models were evaluated for fitness of the sorption data by calculating the sum of squared error (SSE). The SSE values were calculated by the equation:

$$\text{SSE} = \sum \frac{(q_{t,e} - q_{t,m})^2}{q_{t,e}^2} \quad (3)$$

where $q_{t,e}$ and $q_{t,m}$ are the experimental adsorption capacities of bentazon (mg/g) at time t and the corresponding values that are obtained from the kinetic models.

2.5. Desorption studies

Desorption studies were conducted to evaluate the feasibility of regenerating spent LWAC using ethanol desorption technique (Tanthapanichakoon et al., 2005). In an Erlenmeyer flask, 0.05 g of unused LWAC was saturated with bentazon, by contacting with 200 mL of 80 mg/L initial concentration of the herbicide solution. The solution was subsequently agitated in a water-bath shaker at 20 °C and 200 rpm agitation speed for 90 min. The amount of bentazon adsorbed by LWAC was determined from the difference between the initial and the final concentration of this herbicide in the liquid phase. The used LWAC was then filtered and washed gently with distilled water to remove unadsorbed bentazon molecules trapped between the LWAC particles and subsequently dried in an oven at 105 °C for 12 h. The LWAC samples were then mixed

with 200 mL of 95% ethanol and agitated in a water-bath shaker at 20 °C for the same duration as the adsorption test. The concentration of bentazon in the liquid-phase was measured and the amount of herbicide desorbed was determined. The adsorption–desorption cycle was repeated three times using the same LWAC samples. The percent desorption efficiency, D (%) was calculated by comparing the amount of bentazon desorbed with the amount adsorbed from the LWAC for each cycle using Eq. (4):

$$D = \frac{C_{de}}{C_{ad}} \times 100 \quad (4)$$

where C_{de} (mg/L) is the concentration of bentazon at equilibrium in the desorption process and C_{ad} (mg/L) the difference between the initial and equilibrium concentration of this herbicide in the adsorption process.

3. Results and discussion

3.1. Characteristics of LWAC

3.1.1. Specific surface area and pore structure of LWAC

Identifying the pore structure of adsorbent, which is commonly determined by the adsorption of inert gases, is an essential procedure before designing the adsorption process (Tseng et al., 2006). Fig. 2 shows the adsorption–desorption isotherm of N_2 at 77 K. Adsorption data were obtained over the relative pressure, P/P_0 , range from 10^{-7} to 1. Table 1 presents the physical properties of LWAC. The surface area of LWAC was found to be 584 m²/g, which was much higher than conventional activated carbons that is, activated carbons from olive-tree wood revisited (474 m²/g) Ould-Idriss et al., 2011,

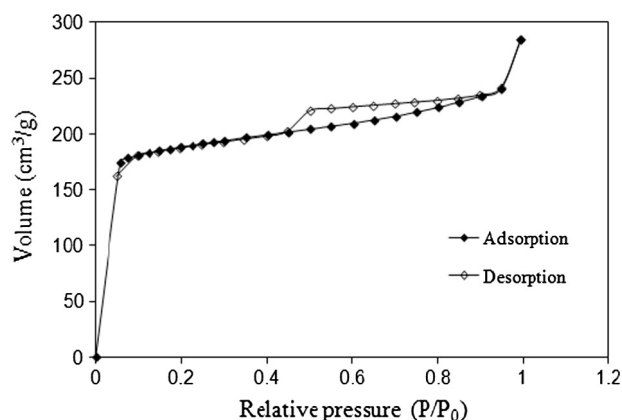


Figure 2 Nitrogen adsorption–desorption isotherms of LWAC.

Table 1 Physical properties of LWAC.

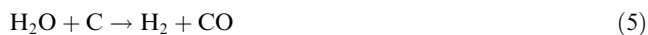
Physical properties	Values
Specific surface area, S_{BET} (m^2/g)	584
Surface area micropore, S_{micro} (m^2/g)	483
External surface area, S_{ext} (m^2/g)	100
Micropore volume, V_{micro} (cm^3/g)	0.245
Total pore volume, V_T (cm^3/g)	0.441

activated carbon from sawdust of Algarroba ($549 \text{ m}^2/\text{g}$) Matos et al., 2011 and wood coal-based activated carbon ($331 \text{ m}^2/\text{g}$) Lorenc-Grabowska and Gryglewicz, 2007.

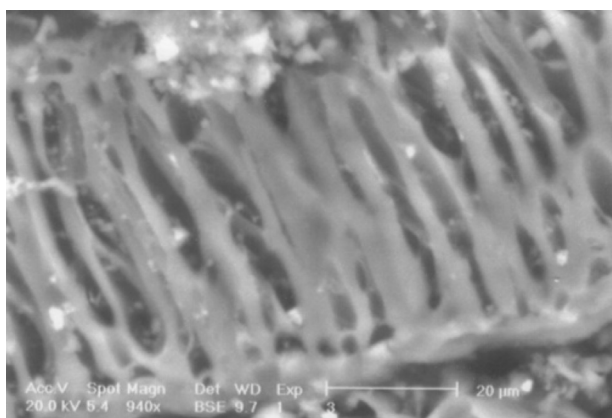
The graph of the adsorption isotherm in Fig. 2, is a Type I isotherm and this indicates that the activated carbon is microporous. Initial step region of the isotherm is abruptly followed by a plateau indicating that the adsorption has virtually stopped because multilayer of adsorbate cannot be formed due to close proximity of the pore wall. It can be seen from Table 1 that most pores of LWAC are in the micropore range, the micropore volume (V_{micro}) occupies the 55% of the total pore volume.

3.1.2. Surface morphology of LWAC

The SEM micrographs of LWAC sample are given in Fig. 3. The external surfaces of these prepared activated carbon show the presence of cavities and are very irregular, indicating that the porosity of the material was produced by attack of the reagent (H_2O) during activation. The increase in the steam tenor supports the following gasification process under high temperature (Tan et al., 2008):



After undergoing carbonization and activation processes, the volatile matter content decreased significantly whereas the fixed carbon content increased in LWAC. This was due to the pyrolytic effect where most of the organic substances have been degraded and discharged as gas and liquid tars leaving a material with high carbon purity (Ahmad et al., 2008). (Adinata et al., 2007) found that increasing the carbonization temperature decreased the yield progressively due to released volatile products as a result of intensifying dehydration and elimination reaction

**Figure 3** SEM image of LWAC.

3.1.3. Function groups of LWAC

The FTIR spectrum of LWAC is illustrated in Fig. 4. A wide absorption band at $3200\text{--}3600 \text{ cm}^{-1}$ with a maximum at about 3411 cm^{-1} is assigned to O–H stretching vibrations of hydrogen bonded hydroxyl groups (Valente Nabais et al., 2011). Aliphatic C–H stretching vibration is found as a very weak peak at 2884 cm^{-1} while asymmetric vibration of CH_2 group appears at 2915 cm^{-1} . The bands located at about 1609 and 1414 cm^{-1} were attributed to carbonyl (e.g. ketone) and carboxylate ion (COO^-) groups, respectively. The shoulder at 1080 cm^{-1} can be ascribed to C–OH stretching of phenolic groups (Figueiredo et al., 1999).

3.2. Effect of adsorbent dosage and initial bentazon concentration

The adsorbent dosage is an important parameter because this parameter determines the capacity of adsorbent for a given bentazon concentration and also determines sorbent–sorbate equilibrium of the system. From the Fig. 5, the removal of bentazon depends on the initial concentration of the adsorbate and the adsorbent dosage. For example, the percentage of removal of bentazon increased for the concentrations 22 mg/L and 78 mg/L , respectively, from 54% and 16.6% at 10 mg to 90.9% and 74.58% at 50 mg of adsorbent dose. The increased removal at high dosages is expected, because of the increased adsorbent surface area and availability of more adsorption sites (Garg et al., 2004, 2003). The optimum dosage was found to be 50 mg . The percentage removal of the bentazon was found to decrease with the increase in initial bentazon concentration at constant amount of adsorbent about 50 mg . This indicates that there exist reductions in immediate solute adsorption, owing to the lack of available active sites required for the high initial concentration of bentazon. Similar results have been reported in the literature (Kannan and Sundaram, 2001; Kilic et al., 2011).

3.3. Effect of stirring rate on bentazon adsorption

The effect of agitation rate on bentazon adsorption is shown in Fig. 6. As the stirring rate increased from 50 to 200 rpm , the adsorption capacity increased from 120.29 to 134.91 mg/g . The decrease in adsorption capacity at a higher shaking rate is probably due to the fact that more particles are broken at 300 rpm , thereby enhancing the desorption process. Another explanation is that the suspension is not homogeneous at 300 rpm (Boualia et al., 1993; Silem et al., 1992; Souza et al., 2007). An agitation speed of 200 rpm was selected for the other tests.

3.4. Effect of pH on bentazon adsorption

Generally, the pH of a solution is recognized as a very influential parameter that governs the adsorption process. It was established that pH affects the surface charge of the adsorbent. The effect of solution pH on the bentazon adsorption was detailed from Fig. 7. The maximum adsorption was determined at pH 3.5 as 136.52 mg/g . The high amount adsorbed of the bentazon solution at acidic pH could be attributed to the complex structure of bentazon (Fig. 1), several adsorptive forces may occur simultaneously. Given the aromatic structure, dispersion forces should be expected between the π electron

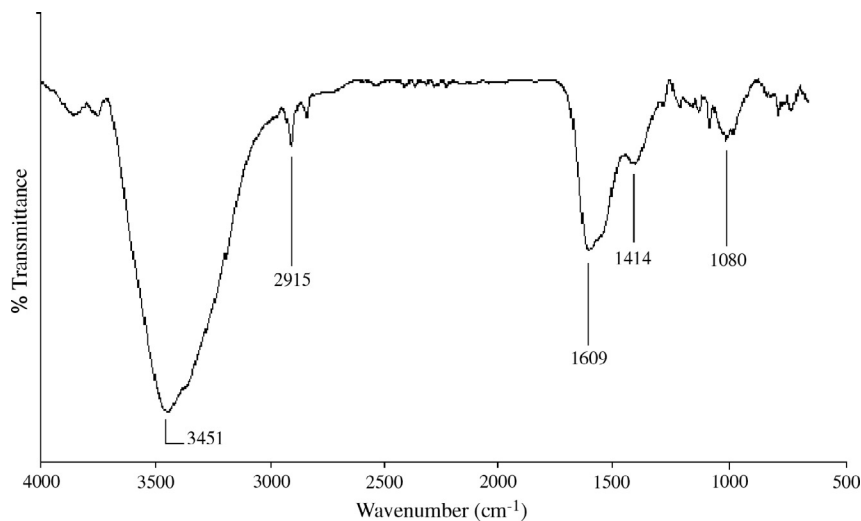


Figure 4 FTIR spectrum of the LWAC.

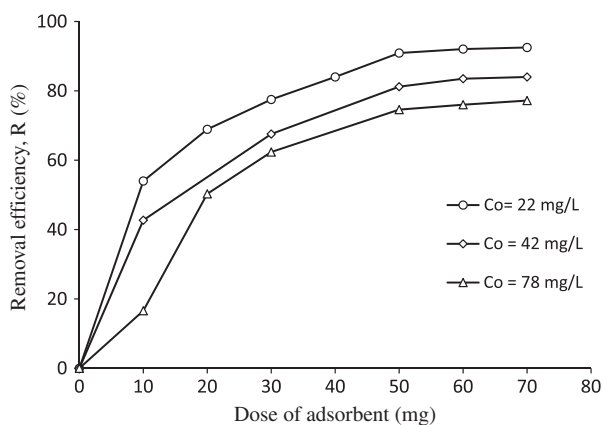


Figure 5 Effect of adsorbent dosage and initial bentazon concentration on bentazon removal onto LWAC (agitation speed = 200 rpm, temperature = 20 °C, pH = 3.5, contact time = 90 min).

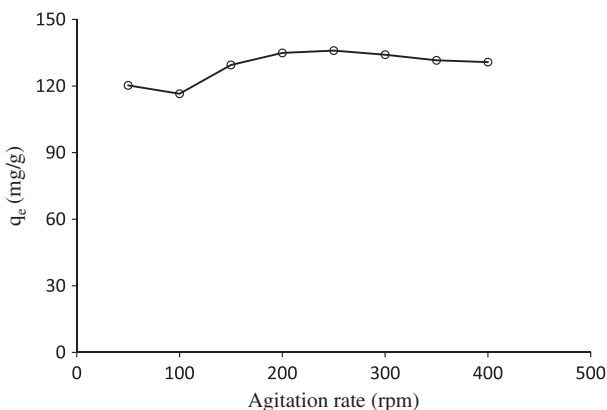


Figure 6 Effect of agitation speed on the adsorption of bentazon onto LWAC (initial bentazon concentration $C_0 = 80$ mg/L, temperature = 20 °C, pH = 3.5, adsorbent dose = 50 mg, contact time = 90 min).

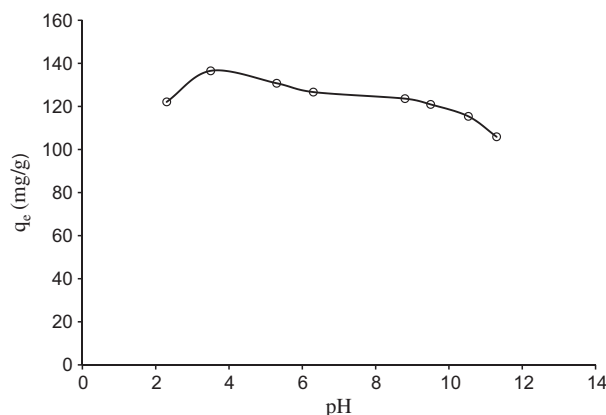


Figure 7 Effect of pH on the adsorption of bentazon onto LWAC (initial bentazon concentration $C_0 = 80$ mg/L, temperature = 20 °C, agitation speed = 200 rpm, adsorbent dose = 50 mg, contact time = 90 min).

density of the graphene layers on the activated carbon and the aromatic ring of the adsorbate. Also, some specific localized interactions might arise from the polar groups (i.e., sulfoxide and carbonyl-type). The decrease in the amount adsorbed at higher pH (anionic form predominant in solution) suggests a weaker interaction of the carbon surface with deprotonated (anionic) bentazon than with its neutral form, and consequently that the adsorption is dominated by dispersive interactions between the pesticide and the adsorbent surface. Similar results on the pH-dependence of bentazon adsorption have been reported (Boivin et al., 2005; Grey et al., 1996).

3.5. Effect of contact time

In order to determine the equilibrium time for maximum uptake, a contact time study was performed with initial concentrations of bentazon of 80 mg/L. A graphical representation of the contact time as given in Fig. 8 suggests that the adsorption increased sharply with contact time in the first 15 min and equilibrium adsorption was established within 90 min. It can

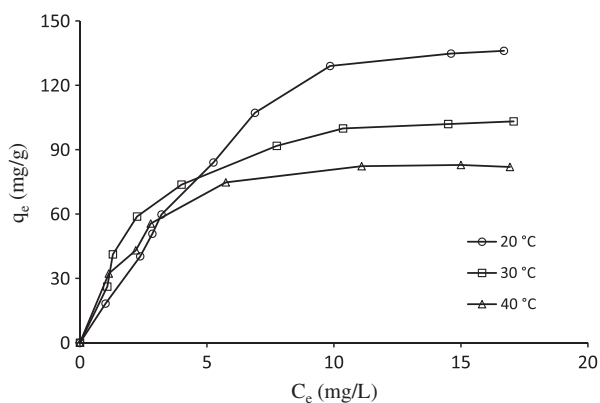


Figure 8 Effect of temperature on the adsorption of bentazon onto LWAC (agitation speed = 200 rpm, adsorbent dose = 50 mg, contact time = 90 min, pH = 3.5).

be seen that the adsorption of bentazon is rapid at the initial stage of the contact period, but it gradually slows down until it reaches equilibrium. The fast adsorption at the initial stage may be due to the fact that a large number of surface sites are available for adsorption. As a result, the remaining vacant surface sites are difficult to be occupied due to formation of repulsive forces between the bentazon molecules on the solid surface and in the bulk phase (Mohd Din et al., 2009). Further increase in contact time did not enhance the adsorption, so, the optimum contact time was selected as 90 min for further experiments.

3.6. Effect of temperature and thermodynamic parameters

Sorption isotherms of bentazon at various temperatures (293–313 K) of solution are shown in Fig. 9. The degree of adsorption decreased with increased temperature, indicating that the adsorption is endothermic. The free energy of adsorption (ΔG°) can be related with the equilibrium constant K_D (L mol^{-1}), the values of enthalpy change (ΔH°) and entropy change (ΔS°), for the adsorption process were calculated, using the following Eqs. (6)–(8):

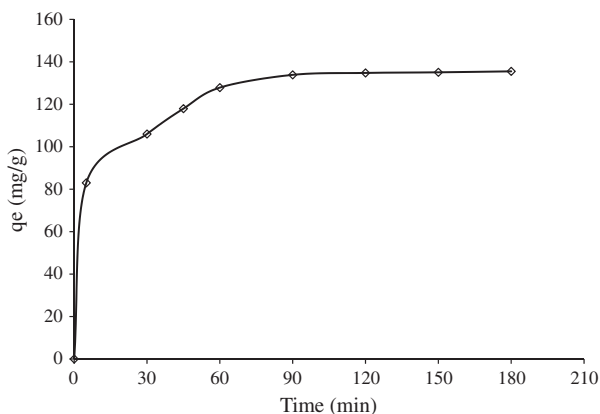


Figure 9 Effect of contact time on the adsorption of bentazon onto LWAC (adsorbent dose = 50 mg, pH = 3.5, concentration $C_0 = 80 \text{ mg/L}$).

$$K_D = \frac{q_e}{C_e} \quad (6)$$

$$\Delta G^\circ = -RT \ln K_D \quad (7)$$

$$\ln K_D = \frac{\Delta S^\circ}{R} - \frac{\Delta H^\circ}{RT} \quad (8)$$

A Van't Hoff plot of $\ln K_D$ as a function of $1/T$ (figure not shown) yields to a straight line. The ΔH° and ΔS° parameters were calculated from the slope and intercept of the plot, respectively. The values of the thermodynamic parameters are listed in Table 2. The negative ΔG° values indicate that process is thermodynamically feasible, spontaneous and chemically controlled. The negative value of ΔH° indicates that the nature of adsorption process is exothermic. This is also supported by the decrease in value of adsorbed capacity of the sorbent with the increase in temperature. The negative value of ΔS° shows the decreased randomness at the solid/solution interface during the adsorption process. Note that this result is in agreement with that reported in paper dealing with adsorption of organic solutes on activated carbons (Kilic et al., 2011).

3.7. Adsorption isotherms

Several equilibrium models have been used to describe the equilibrium nature of adsorption. The Langmuir, Freundlich and Temkin isotherm are the most frequently used models to describe the adsorption data. Langmuir model is based on the assumption that adsorption energy is constant and independent of surface coverage. The maximum adsorption occurs when the surface is covered by a monolayer of adsorbate. The Langmuir isotherm (Langmuir, 1918) is given by Eq. (9):

$$q_e = \frac{Q_m b C_e}{1 + b C_e} \quad (9)$$

The linear form of Langmuir isotherm equation is given as:

$$\frac{C_e}{q_e} = \frac{1}{Q_m b} + \frac{C_e}{Q_m} \quad (10)$$

Table 2 Isotherm constants and thermodynamic parameters for bentazon adsorption onto LWAC at different temperatures.

	Temperatures		
	293 K	303 K	313 K
<i>Langmuir isotherm</i>			
Q_m (mg/g)	169.491	104.166	89.956
b (L/mg)	0.183	0.510	0.672
R_L	0.063	0.023	0.018
R^2	0.969	0.997	0.997
<i>Freundlich isotherm</i>			
K_F (mg/g) (L/mg) ^{1/n}	27.631	42.014	43.906
n	1.615	2.896	2.912
R^2	0.934	0.951	0.910
<i>Temkin isotherm</i>			
b_T (J/mol)	22.420	44.782	57.968
A (L/g)	1.085	1.958	2.052
R^2	0.971	0.983	0.942
<i>Thermodynamic parameters</i>			
ΔG° (kJ/mol)	-16.640	-13.399	-12.740
ΔS° (kJ/mol K)		-0.207	
ΔH° (kJ/mol)		-77.233	

where C_e is the equilibrium concentration of the adsorbate (mg/L), q_e is the amount of adsorbate adsorbed per unit mass of adsorbent (mg/g), b is the Langmuir adsorption constant (L/mg), and Q_m is the theoretical maximum adsorption capacity (mg/g).

The essential characteristics of Langmuir equation can be expressed in terms of dimensionless separation factor, R_L , defined as (Weber and Chakkravorti, 1974):

$$R_L = \frac{1}{(1 + bC_0)} \quad (11)$$

where b is the Langmuir isotherm constant (L/mg) and C_0 is the initial bentazon concentration (mg/L). The R_L value indicates the type of the isotherm to be either favorable ($0 < R_L < 1$), unfavorable ($R_L > 1$), linear ($R_L = 1$) or irreversible ($R_L = 0$).

Freundlich model is based on sorption on a heterogeneous surface of varied affinities (Freundlich, 1906). The logarithmic form of Freundlich was given as:

$$\log q_e = \log K_F + \left(\frac{1}{n}\right) \log C_e \quad (12)$$

where K_F and n are Freundlich constants with n as a measure of deviation of the model from linearity of the adsorption and K_F (mg/g (L/mg)^{1/n}) indicates the adsorption capacity of the adsorbent.

Temkin isotherm based on the heat of adsorption of the ions, which is due to the adsorbate and adsorbent interactions taken in linear form, is given by Choy et al. (1999):

$$q_e = \left(\frac{RT}{b_T}\right) \ln A + \left(\frac{RT}{b_T}\right) \ln C_e \quad (13)$$

where $B = RT/b_T$, b_T is the Temkin constant related to the heat of sorption (J/mol), A is the Temkin isotherm constant (L/g), R the gas constant (8.314 J/mol K) and T the absolute temperature (K).

The linear plot of specific adsorption (C_e/q_e) against the equilibrium concentration (C_e) for Langmuir model, ($\log q_e$) against the ($\log C_e$) for Freundlich model and (q_e) against the ($\ln C_e$) for Temkin models is shown in Figs. 10–12.

Table 2 summarizes all the constants and correlation coefficient, R^2 values obtained from the three isotherm models ap-

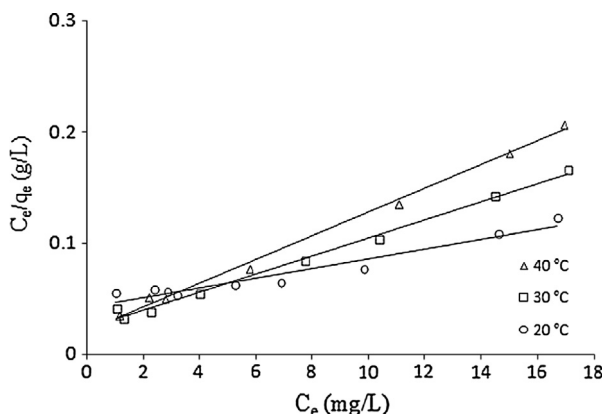


Figure 10 Langmuir isotherm plots for adsorption of bentazon onto LWAC at different temperatures (temperature = 20, 30 and 40 °C; agitation speed = 200 rpm, adsorbent dose = 50 mg, contact time = 90 min, pH = 3.5).

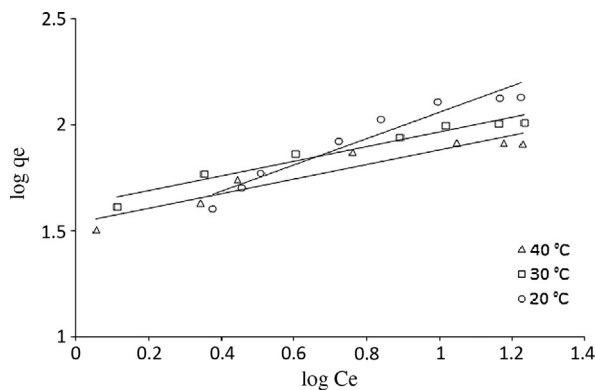


Figure 11 Freundlich isotherm plots for adsorption of bentazon onto LWAC at different temperatures (temperature = 20, 30 and 40 °C; agitation speed = 200 rpm, adsorbent dose = 50 mg, contact time = 90 min, pH = 3.5).

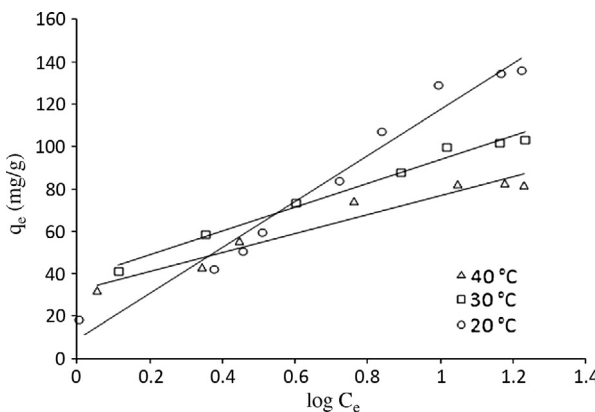


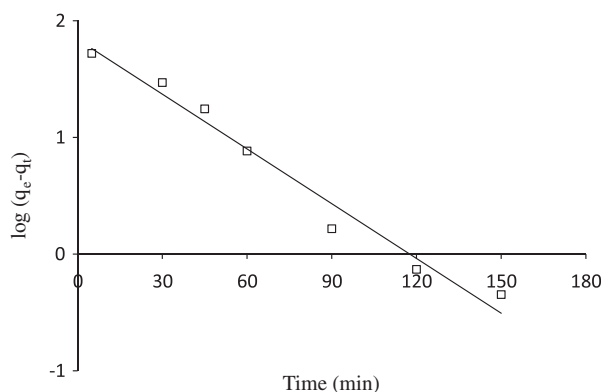
Figure 12 Temkin isotherm plots for adsorption of bentazon onto LWAC at different temperatures (temperature = 20, 30 and 40 °C; agitation speed = 200 rpm, adsorbent dose = 50 mg, contact time = 90 min, pH = 3.5).

plied for adsorption of bentazon from aqueous solutions on the LWAC. From Table 2, the values of n were found to be less than 10 and the values of R_L were in the range of 0.018–0.063 indicating that the adsorption was favorable. According to Trybal (Trybal, 1980) it has been shown using mathematical calculations that n values between 1 and 10 represent beneficial adsorption. The Langmuir isotherms were found to be linear over the whole concentration range studied and the correlation coefficients R^2 , were extremely high compared to the Freundlich and Temkin isotherms, indicating that the Langmuir isotherm better represented the experimental adsorption data at all solution temperatures. As can be further seen from Table 2, the values of Q_m decreased with temperature, indicating that the adsorption process was exothermic in nature.

Table 3 compares the maximum adsorption capacity of LWAC with various adsorbents reported in the literature for the adsorptive removal of bentazon. Though there were variations in some experimental conditions, the table shows that the adsorption capacity of LWAC for this herbicide is high compared to other activated carbons used in previous studies. The bentazon adsorption capacity exhibited by LWAC shows that Lawsonia inermis wood is a good precursor for the

Table 3 Compared performances of LWAC and other adsorbents with standard discharge limit of bentazon.

Standard discharge limit	Adsorbent	Initial concentration (mg/L)	Q_m (mg/g)	Reference
≤0.3 mg/L	Garden waste compost	1–250	54.67	Wilde et al. (2009)
	Coco chips	1–250	0.15	Wilde et al. (2009)
	Oxidized activated carbon cloth	50–200	17	Ania and Beguin (2007)
	Banana stalk-based activated carbon	25–250	115.07	Salman et al. (2011a)
	Date seed-based activated carbon	25–250	86.26	Salman et al. (2011b)
	Activated carbon cloth	50–200	151	Ayranci and Hoda (2004)
	Lawsonia inermis wood-based activated carbon	20–80	169.491	This study

**Figure 13** Pseudo-first-order kinetic plot for the adsorption of bentazon onto LWAC (temperature = 20 °C; agitation speed = 200 rpm, adsorbent dose = 50 mg, min, pH = 3.5, concentration $C_0 = 80$ mg/L).

preparation of activated carbon for the adsorptive removal bentazon. For aqueous solutions of bentazon having lower concentrations than 170 mg/L, the totality of this herbicide is eliminated by using one gram of activated carbon and thereafter these treated concentrations can be admitted by the USEP-A in drinking water.

3.8. Adsorption kinetics

In this study, the adsorption equilibrium data were analyzed using three kinetic models, pseudo-first-order, pseudo-second-order and intraparticle diffusion model. The pseudo-first-order equation can be expressed as (Hameed et al., 2007):

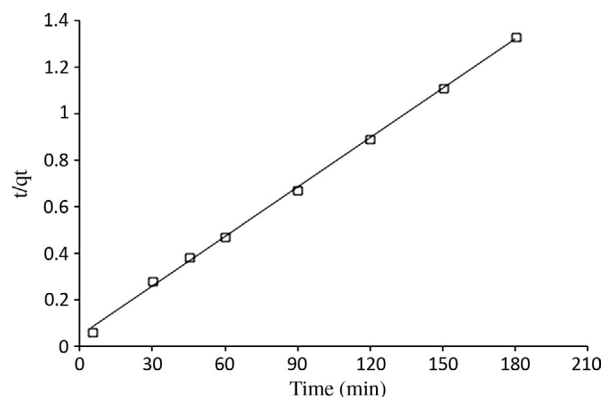
$$\log(q_e - q_t) = \log q_e - \frac{k_1}{2.303} t \quad (14)$$

where q_e and q_t are the amounts adsorbed at equilibrium and at time t (mg/g), and k_1 is the rate constant of the pseudo-first-order adsorption (min^{-1}). The linear plot of $\log(q_e - q_t)$ versus t gives a slope of k_1 and intercept of $\log q_e$ as shown in Fig. 13.

The pseudo-second-order kinetic model can be represented in the following form (Franca et al., 2009):

$$\frac{t}{q_t} = \frac{1}{k_2 q_e^2} + \frac{1}{q_e} t \quad (15)$$

where k_2 (g/mg min) is the rate constant of second-order adsorption. The linear plot of t/q_t versus t gave $1/q_e$ as the slope and $1/k_2 q_e^2$ as the intercept. Fig. 14 shows a good agreement between the experimental and the calculated q_e values.

**Figure 14** Pseudo-second-order kinetic plot for the adsorption of bentazon onto LWAC (temperature = 20 °C; agitation speed = 200 rpm, adsorbent dose = 50 mg, min, pH = 3.5, concentration $C_0 = 80$ mg/L).

The rate constants and R^2 values are given in Table 4. However, the correlation coefficients, R^2 , showed that the pseudo-second-order model fits better with the experimental data than the pseudo-first order model. In addition, the sum of squared error (SSE) test was also done to support the best fit adsorption model (Table 4). SSE values were lower for pseudo-second-order model than the pseudo-first order model. Based on R^2 and SSE values it was confirmed that pseudo-second-order model best fits the adsorption data, an indication of chemisorption mechanism. The results are also analyzed in terms of intraparticle diffusion model to investigate whether the intraparticle diffusion is the rate controlling step in adsorption of bentazon onto LWAC.

The intraparticle diffusion equation is expressed as (Weber and Morris, 1963):

$$q_t = k_{\text{int}} t^{1/2} + C \quad (16)$$

Where k_{int} is the intraparticle diffusion rate constant ($\text{mg/g min}^{1/2}$) and C is the intercept, which represents the thickness of the boundary layer. If intra-particle diffusion occurs, then q_t versus $t^{1/2}$ will be linear and if the plot passes through the origin, then the rate limiting step is only due to the intra-particle diffusion. Otherwise, this plot gives general features of three stages: initial curved portion, followed by an intermediate linear portion and a plateau. The initial sharper, is due to the instantaneous adsorption or external surfacing adsorption (external mass transfer). The intermediate linear part is due to intra-particle diffusion and the plateau to the equilibrium stage where intraparticle diffusion starts to slow down due to

Table 4 Kinetic model parameters for adsorption of bentazon onto LWAC.

Kinetic model	Parameter	Value
Pseudo-first-order	$q_e, \text{ exp (mg/g)}$	135.07
	$q_e, \text{ cal (mg/g)}$	69.199
	$k_1 \text{ (min}^{-1}\text{)}$	0.035
	R^2	0.973
	SSE	0.998
Pseudo-second-order	$q_e, \text{ cal (mg/g)}$	140.845
	$k_2 \text{ (g mg}^{-1}\text{min)}$	0.001
	R^2	0.998
	SSE	0.644
Intraparticle diffusion model	$k_{\text{int}} \text{ (g/mg min)}$	8.057
	R^2	0.993

extremely low solute concentrations in the solution (Daifullah et al., 2007).

Plot of the quantity of bentazon adsorbed against square root of time is shown in Fig. 15. It can be observed that the plots are not linear over the whole time range and the graphs of this figure reflect a dual nature, with initial linear portion followed by a plateau. The fact that the first curved portion of the plots seems to be absent which implies that the external surface adsorption (stage 1) is relatively very fast and the stage of intra-particle diffusion (stage 2) is rapidly attained and continued to 90 min. Finally, equilibrium adsorption (stage 3) starts after 90 min. The bentazon molecules are slowly transported via intra-particle diffusion into the particles and are finally retained in the pores. The results obtained agreed with those found by Monser and Adhoum(2009) for the adsorption of tartrazine onto activated carbon. The values of k_{int} and C were determined from the slopes of the linear plots, and the constants of intraparticle diffusion model are given in Table 4.

3.9. Batch adsorption process design

The design of batch adsorption systems can be predicted using adsorption isotherms (Ozacar and Sengil, 2004). The design

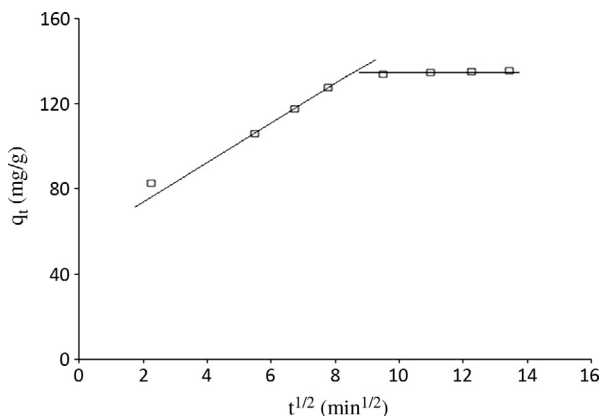


Figure 15 Intraparticle diffusion plots for adsorption of bentazon onto LWAC (temperature = 20 °C; agitation speed = 200 rpm, adsorbent dose = 50 mg, min, pH = 3.5, concentration $C_0 = 80 \text{ mg/L}$).

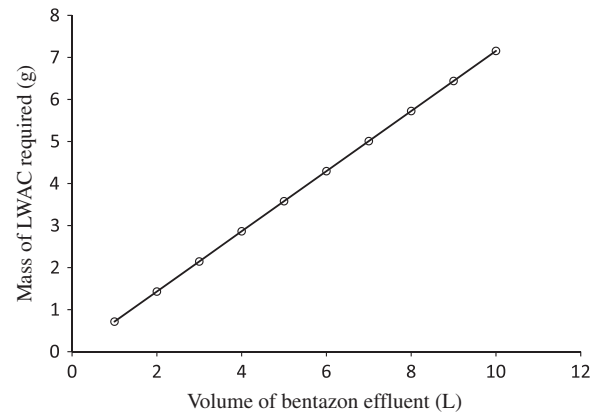


Figure 16 Variation of mass of LWAC required with volume of bentazon effluent to be treated for 90% removal efficiency of bentazon of initial concentration 80 mg/L at 20 °C.

Table 5 Percent desorption of bentazon from herbicide-loaded LWAC by ethanol.

Herbicide	Percent desorption efficiency (%)		
	1st cycle	2nd cycle	3rd cycle
Bentazon	78.3	76.1	73.8

objective is to reduce the bentazon solution of volume V (L) from an initial concentration of C_0 to C_e (mg/L) for a single-stage batch adsorption system. The mass of LWAC required is m (g), and the herbicide loading on LWAC changes from q_0 to q_e (mg/g). At $t = 0$, $q_0 = 0$ and as time proceeds the mass balance equates the herbicide removed from solution to that adsorbed on LWAC as expressed in Eq. (17):

$$V(C_0 - C_e) = m(q_e - q_0) = mq_e \quad (17)$$

The adsorption isotherm studies confirmed that the Langmuir isotherm equation was more applicable and described the adsorption data more adequately. Therefore, substituting Eq. (9) into Eq. (17) and rearranging, Eq. (18) was obtained:

$$m = \frac{V(C_0 - C_e)(1 + bC_e)}{Q_m b C_e} \quad (18)$$

Rearranging Eq. (2), we obtained Eqs. (19) and (20):

$$C_0 - C_e = \frac{RC_0}{100} \quad (19)$$

$$C_e = C_0 \left(1 - \frac{R}{100}\right) \quad (20)$$

Substituting Eqs. (19) and (20) into Eq. (18), we obtained Eq. (21):

$$m = \frac{VRC_0(1 + b(C_0(1 - \frac{R}{100})))}{100Q_m b(C_0(1 - \frac{R}{100}))} \quad (21)$$

Eq. (21) was used to calculate the mass m (g) of LWAC required to achieve any given percent removal efficiency (R) from aqueous solution of volume V (L) for any given initial concentration of bentazon C_0 (mg/L), except for 100% removal conditions. Fig. 16 shows the plot of calculated mass of LWAC required to remove bentazon solution of initial

concentration 80 mg/L to achieve 90% removal efficiency for different solution volumes (1–10 L) at 20 °C for a single-stage batch adsorption system. The amount of adsorbent required increased with the volume of solution to be treated.

3.10. Desorption studies

Table 5 shows the percent desorption efficiency of bentazon from the herbicide-loaded LWAC for three cycles. High percent desorption efficiency was obtained with value of 73.8% after three cycles. The good result obtained implies that LWAC is reusable for bentazon adsorption. The higher percent desorption efficiency obtained for bentazon in each cycle could be attributed to stronger attachment between prepared activated carbon and herbicide, which is in accord with our previous observations in this study.

4. Conclusions

The present study focused on adsorption of bentazon from aqueous solution using the *Lawsonia inermis* wood-based activated carbon as a low cost adsorbent. The external surfaces of these prepared activated carbon show the presence of cavities and are very irregular. The surface area of the adsorbent was found to be 584 m²/g. The adsorption characteristic has been examined with the variations in the parameters of pH, contact time, activated carbon dosage, stirring rate, initial bentazon concentration and temperature. The experimental data were analyzed using Langmuir, Freundlich and Temkin isotherm models. The Langmuir model provides the best correlation of the experimental equilibrium data. The adsorption capacity of the activated carbon was determined as 169.49 mg/g at 20 °C. The adsorption system obeys the pseudo-second order kinetic model. The adsorption mechanism of this herbicide is rather a complex process and the intra-particle diffusion was not the only rate-controlling step. Thermodynamic parameters suggested that the adsorption of bentazon on the *Lawsonia inermis* wood activated was feasible, spontaneous and exothermic in nature.

Acknowledgements

The authors thank the Scientific Research Projects Unit of Valorization of the Useful Substances (ENIS) for the support of this work through the project. Also, they thank Mm. Asma BEN ABDELLAH for this linguistic assistance in this manuscript.

References

- Adinata, D., Wan Daud, W.M.A., Aroua, M.K., 2007. Preparation and characterization of activated carbon from palm shell by chemical activation with K₂CO₃. *Bioresour. Technol.* 98, 145–149.
- Ahmad, A.L., Tan, L.S., Shukor, S.R.A., 2008. Dimethoate and atrazine retention from aqueous solution by nanofiltration membranes. *J. Hazard. Mater.* 151, 71–77.
- Ahmad, M.A., Wan Daud, W.M.A., Aroua, M.K., 2008. CO₂/CH₄ and O₂/N₂ kinetic selectivities of oil palm shell based carbon molecular sieves. *J. Oil Palm Res.* 20, 453–460.
- Ali, I., Gupta, V.K., 2006. Advances in water treatment by adsorption technology. *Nat. Protoc.* 1, 2661–2667.
- Ali, S., Hussain, T., Nawaz, R., 2009. Optimization of alkaline extraction of natural dye from Henna leaves and its dyeing on cotton by exhaust method. *J. Cleaner Prod.* 17, 61–66.
- Al-Sehaibani, H., 2000. Evaluation of extraction of Henna leaves as environmentally friendly corrosion inhibitor for metals. *Material-wissenschaft Werkstofftech* 31, 1060–1063.
- Ania, C.O., Beguin, F., 2007. Mechanism of adsorption and electro-sorption of bentazon on activated carbon cloth in aqueous solutions. *Water Res.* 41, 3372–3380.
- Aungradit, T., Sutthivaiyakit, P., Martens, D., Sutthivaiyakit, S., Kettrup, A.A.F., 2007. Photocatalytic degradation of triazophos in aqueous titanium dioxide suspension: identification of intermediates and degradation pathways. *J. Hazard. Mater.* 146, 204–213.
- Ayranci, E., Hoda, N., 2004. Adsorption of bentazon and propanil from aqueous solutions at the high area activated carbon-cloth. *Chemosphere* 57, 755–762.
- Ballesteros Martin, M.M., Sanchez Perez, J.A., Garcia Sanchez, J.L., Montes de Oca, L., Casas Lopez, J.L., Oller, I., Malato Rodriguez, S., 2008. Degradation of alachlor and pyrimethanil by combined photo-Fenton and biological oxidation. *J. Hazard. Mater.* 155, 342–349.
- Boivin, A., Cherrier, R., Schiavon, M., 2005. A comparison of five pesticides adsorption and desorption processes in thirteen contrasting field soils. *Chemosphere* 61, 668–676.
- Boualia, A., Mellah, A., Aissaoui, T.T., Menacer, K., Silem, A., 1993. Adsorption of organic matter contained in industrial H₃PO₄ onto bentonite: batch-contact time and kinetic study. *Appl. Clay Sci.* 7, 431–445.
- Choy, K.K.H., McKay, G., Porter, J.F., 1999. Sorption of acid dyes from effluents using activated carbon. *Resour. Conserv. Recycl.* 27, 57–71.
- Chung, W.H., Chang, Y.C., Yang, L.J., Hung, S.I., Wong, W.R., Lin, J.Y., et al., 2002. Clinicopathologic features of skin reactions to temporary tattoos and analysis of possible causes. *Arch. Dermatol.* 88, 138.
- Daifullah, A.A.M., Yakout, S.M., Elreefy, S.A., 2007. Adsorption of fluoride in aqueous solutions using KMnO₄-modified activated carbon derived from steam pyrolysis of rice straw. *J. Hazard. Mater.* 147, 633–643.
- Dweck, A.C., 2002. Natural ingredients for colouring and styling. *Int. J. Cosmet. Sci.* 24, 287–302.
- Figueiredo, J.L., Pereira, M.F.R., Freitas, M.M.A., Órfão, J.J.M., 1999. Modification of the surface chemistry of activated carbons. *Carbon* 37, 1379–1389.
- Franca, A.S., Oliveira, L.S., Ferreira, M.E., 2009. Kinetics and equilibrium studies of methylene blue adsorption by spent coffee grounds. *Desalination* 249, 267.
- Freundlich, H.M.F., 1906. Over the adsorption in solution. *J. Phys. Chem.* 57, 385–470.
- Garg, V.K., Gupta, R., Yadav, A.B., Kumar, R., 2003. Dye removal from aqueous solution by adsorption on treated saw dust. *Bioresour. Technol.* 89, 121–124.
- Garg, V.K., Kumar, R., Gupta, R., 2004. Removal of malachite green dye from aqueous solution by adsorption using agro-industry waste: a case study of *Prosopis cineraria*. *J. Dyes Pigm.* 62, 1–10.
- Garrido, M., Lima, C., Matos, D., Brett, O., 1998. Electrochemical oxidation of bentazon at a glassy carbon electrode application to the determination of a commercial herbicide. *Talanta* 46, 1131–1135.
- Grey, T.L., Wehtje, G.R., Walker, R.H., Hajek, B.H., 1996. Sorption and mobility of bentazon in coastal plain soils. *Weed Sci.* 44, 166–170.
- Halim, A.A., Aziz, H.A., Johari, M.A.M., Ariffin, K.S., 2010. Comparison study of ammonia and COD adsorption on zeolite, activated carbon and composite materials in landfill leachate treatment. *Desalination* 262, 31–35.

- Hameed, B.H., Ahmad, A.L., Latiff, K.N.A., 2007. Adsorption of basic dye (methylene blue) onto activated carbon prepared from rattan sawdust. *Dyes Pigm.* 75, 143.
- Kannan, N., Sundaram, M.M., 2001. Kinetics and mechanism of removal of methylene blue by adsorption on various carbons – a comparative study. *Dyes Pigm.* 51, 25–40.
- Kilic, M., Apaydin-Varol, E., Putun, A.E., 2011. Adsorptive removal of phenol from aqueous solutions on activated carbon prepared from tobacco residues: equilibrium, kinetics and thermodynamics. *J. Hazard. Mater.* 189, 397–403.
- Kilic, M., Apaydin-Varol, E., Ays, Putun, E., 2011. Adsorptive removal of phenol from aqueous solutions on activated carbon prepared from tobacco residues: equilibrium, kinetics and thermodynamics. *J. Hazard. Mater.* 189, 397–403.
- Langmuir, I., 1918. The adsorption of gases on plane surfaces of glass, mica and platinum. *J. Am. Chem. Soc.* 40, 1361–1403.
- Lorenc-Grabowska, E., Gryglewicz, G., 2007. Adsorption characteristics of Congo red on coal-based mesoporous activated carbon. *J. Dyes Pigm.* 74, 34–40.
- Mahalakshmi, M., Arabindoo, B., Palanichamy, M., Murugesan, V., 2007. Photocatalytic degradation of carbofuran using semiconductor oxides. *J. Hazard. Mater.* 143, 240–245.
- Maldonado, M.I., Malato, S., Perez-Estrada, L.A., Gernjak, W., Oller, I., Domenech, X., Peral, J., 2006. Partial degradation of five pesticides and an industrial pollutant by ozonation in a pilot-plant scale reactor. *J. Hazard. Mater.* 38, 363–369.
- Matos, J., Nahas, C., Rojas, L., Rosales, M., 2011. Synthesis and characterization of activated carbon from sawdust of Algarroba wood. I. Physical activation and pyrolysis. *J. Hazard. Mater.* 196, 360–369.
- Mohd Din, A.T., Hameed, B.H., Ahmad, A.L., 2009. Batch adsorption of phenol onto physiochemical-activated coconut shell. *J. Hazard. Mater.* 161, 1522–1529.
- Monser, L., Adhoum, N., 2009. Tartrazine modified activated carbon for the removal of Pb(II), Cd(II) and Cr(III). *J. Hazard. Mater.* 16, 263–269.
- Mourão, P.A.M., Laginhas, C., Custódio, F., Nabais, J.M.V., Carrott, P.J.M., Ribeiro Carrott, M.M.L., 2011. Influence of oxidation process on the adsorption capacity of activated carbons from lignocellulosic precursors. *Fuel Process. Technol.* 92, 241–246.
- Navalon, A., Prielo, A., Araujo, L., Vilchez, J.L., 2002. Determination of oxadiazon residues by headspace solid-phase micro-extraction and gas chromatography-mass spectrometry. *J. Chromatogr. A* 946, 239–245.
- Ould-Idriss, A., Stitou, M., Cuerda-Correa, E.M., Fernández-González, C., Macías-García, A., Alexandre-Franco, M.F., Gómez-Serrano, V., 2011. Preparation of activated carbons from olive-tree wood revisited. II. Physical activation with air. *Fuel Process. Technol.* 92, 266–270.
- Ozcar, M., Sengil, I.A., 2004. Equilibrium data and process design for adsorption of disperse dyes onto alunite. *Environ. Geol.* 45, 762–768.
- Pourata, R., Khataee, A.R., Aber, S., Daneshvar, N., 2009. Removal of the herbicide bentazon from contaminated water in the presence of synthesized nanocrystalline TiO₂ powders under irradiation of UV-C light. *Desalination* 249, 301–307.
- Rajashekara Murthy, H.M., Manonmani, H.K., 2007. Aerobic degradation of technical hexachlorocyclohexane by a defined microbial consortium. *J. Hazard. Mater.* 149, 18–25.
- Ren, L., Zhang, J., Li, Y., Zhang, C., 2011. Preparation and evaluation of cattail fiber-based activated carbon for 2,4-dichlorophenol and 2,4,6-trichlorophenol removal. *Chem. Eng. J.* 168, 553–561.
- Salman, J.M., Njoku, V.O., Hameed, B.H., 2011a. Adsorption of pesticides from aqueous solution onto banana stalk activated carbon. *Chem. Eng. J.* 174, 41–48.
- Salman, J.M., Njoku, V.O., Hameed, B.H., 2011b. Bentazon and carbofuran adsorption onto date seed activated carbon: kinetics and equilibrium. *Chem. Eng. J.* 173, 361–368.
- Saritha, P., Aparna, C., Himabindu, V., Anjaneyulu, Y., 2007. Comparison of various advanced oxidation processes for the degradation of 4-chloro-2 nitrophenol. *J. Hazard. Mater.* 149, 609–614.
- Silem, A., Boualia, A., Kada, R., Mellah, A., 1992. Adsorption of organic matter from a wet phosphoric acid using activated carbon: batch contact time study and linear driving force models. *Can. J. Chem. Eng.* 70, 491–498.
- Souza, A.D., Pina, P.S., Leao, V.A., Silva, C.A., Siqueira, P.F., 2007. The leaching kinetics of a zinc sulphite concentrate in acid ferric sulphate. *Hydrometallurgy* 89, 72–81.
- Tan, I.A.W., Ahmad, A.L., Hameed, B.H., 2008. Preparation of activated carbon from coconut husk: optimization study on removal of 2,4,6-trichlorophenol using response surface methodology. *J. Hazard. Mater.* 153, 709–717.
- Tanthapanichakoon, W., Ariyadejanich, P., Japthong, P., Nakagawa, K., Mukai, S.R., Tamon, H., 2005. Adsorption-desorption characteristics of phenol and reactive dyes from aqueous solution on mesoporous activated carbon prepared from waste tires. *Water Res.* 39, 1347–1353.
- Trybal, R.E., 1980. *Mass Transfers Operations*, third ed. McGraw, New York.
- Tseng, R.L., Tseng, S.K., Wu, F.C., 2006. Preparation of high surface area carbons from corncob with KOH etching plus CO₂ gasification for the adsorption of dyes and phenols from water. *Colloid Surf. A* 279, 69–78.
- United States Environmental Protection Agency (USEPA), 1996. *Drinking Water Standards and Health Advisories*. EPA 822-R-96-001. Office of Water, USEPA, Washington, DC.
- Valente Nabais, J.M., Laginhas, C.E.C., Carrott, P.J.M., Ribeiro Carrott, M.M.L., 2011. Production of activated carbons from almond shell. *Fuel Process. Technol.* 92, 234–240.
- Wang, S.L., Tzou, Y.M., Lu, Y.H., Sheng, G., 2007. Removal of 3-chlorophenol from water using rice-straw-based carbon. *J. Hazard. Mater.* 147, 313–318.
- Weber, T.W., Chakkavorti, R.K., 1974. Pore and solid diffusion models for fixed-bed adsorbers. *AIChE J.* 20, 228–238.
- Weber, W.J., Morris, J.C., 1963. Kinetics of adsorption on carbon from solution. *J. Sanit. Eng. Div.: Am. Soc. Civ. Eng.* 89, 31–59.
- Wilde, T.D., Spanoghe, P., Ryckeboer, J., Jaeken, P., Springael, D., 2009. Sorption characteristics of pesticides on matrix substrates used in biopurification systems. *Chemosphere* 75, 100–108.
- World Health Organisation (WHO), 2004. *WHO Guidelines for Drinking-Water Quality*. World Health Organisation (WHO), Geneva.